

SPACE CHARGE AND COHERENT EFFECTS IN THE NSNS STORAGE RING *

RECEIVED

CONF-960621-^b JUL 15 1996

A.G. Ruggiero, W.T. Weng, S.Y. Zhang
AGS Department - Brookhaven National Laboratory - Upton, NY 11973, USA

OSTI

1 INTRODUCTION

The goal of the proposed National Spallation Neutron Source (NSNS) [1] is to provide a short pulse proton beam of about 0.5 μ s with average beam power of 1-2 MW. To achieve such a purpose, a proton storage ring operated at 60 Hz with 1.2×10^{14} protons per pulse at 1 GeV is required.

The proton storage ring is one of the major systems in the design of the NSNS. The function of the storage ring is to take the 1.0 GeV proton beam from the Linac and convert the long Linac beam of about 1 ms into a 0.5 μ s beam in about one thousand turns. The final beam has 1×10^{14} proton per pulse, resulting in 1 MW average beam power at 60 Hz repetition rate. Provision has been reserved for a future upgrade to 2 MW by doubling the storage beam to 2×10^{14} proton per pulse. The lattice of the storage ring is a simple FODO lattice with three-fold symmetry and the dispersion function is reduced to zero at straight sections by the missing magnet scheme. The total circumference of the ring is 208.6 m and the transition energy is 3.43, higher than the operating energy of 1 GeV to avoid the difficult instability problem that are expected above transition. Other salient design parameters are shown in Table 1.

2 WALL IMPEDANCE BUDGET

The frequency range and the magnitude of the wall-coupling impedance in a storage ring is determined essentially by the dimensions of the vacuum chamber and by the energy of the beam through the relativistic factor γ . A major feature of a low-energy storage ring is the low value of γ and therefore of the impedance frequency range of interest. In fact the cut-off harmonic number above which the beam does not interact effectively with the wall components is given roughly by $n_c \sim \gamma R/b$, where R is the average ring radius and b is the average vacuum chamber size. Using parameters shown in Table 1 it is seen that $n_c \sim 277$, which is a very narrow frequency range (of only 0.5 GHz).

3.1 Longitudinal Coupling Impedance

It is customary [2] to express the beam-wall interaction by the Z/n impedance because it enters in some stability con-

ditions. The space-charge contribution, that is the electromagnetic field stored in the region between the beam and the vacuum chamber, is then [3]

$$Z/n = i Z_0 (1 + 2 \ln b/a) / 2 \beta^2 \quad (1)$$

where $Z_0 = 377$ ohm and a is the average beam radius. For the example given in Table 1, the space-charge contribution is 114 i ohm.

Table 1: General Parameters of the NSNS Project

Average Power	1.0 MW	2.0 MW
Kinetic Energy	1.0 GeV	
Number of Protons	1.04×10^{14}	2.08×10^{14}
Betatron Tunes, H / V	3.82 / 3.78	
Full Betatron Emittance	$60 \pi \text{ mm mrad}$	$120 \pi \text{ mm mrad}$
RF peak Voltage (h = 1)	13 kV	26 kV
Revolution Frequency	1.258 MHz	
Filling Time	1.0 ms	
Synchrotron Period	1.7 ms	1.2 ms
Bunching Factor	0.324	
Bunch Area	7 eV-s	10 eV-s
Full Momentum Spread	1.2 %	1.7 %
Average Pipe Radius	12 cm	

The next contribution is the resistivity of the wall [4]

$$Z/n = (1 - i) (Z_0 \rho_w R / 2 b^2 n)^{-1/2} \quad (2)$$

where the wall resistivity $\rho_w = 2.83 \mu\Omega \times \text{cm}$ for Aluminum. At the lowest harmonic $n=1$, we have $Z/n = (1-i) 0.12$ ohm. At the same time the skin depth is 0.0744 mm. Thus a vacuum chamber thickness of 2 mm is more than adequate for screening the beam from interacting with other components outside the vacuum chamber.

Next we have contributions which are caused by discontinuity of the vacuum chamber. These are bellows, beam position monitors, vacuum chamber steps, pump ports, kicker magnets, and rf cavities. Explicit expressions and contribution from each of them can be found in [5].

* Work performed under the auspices of the U.S. Department of Energy

Figure 1 gives a plot of the expected total longitudinal coupling impedance for the example of the NSNS storage ring.

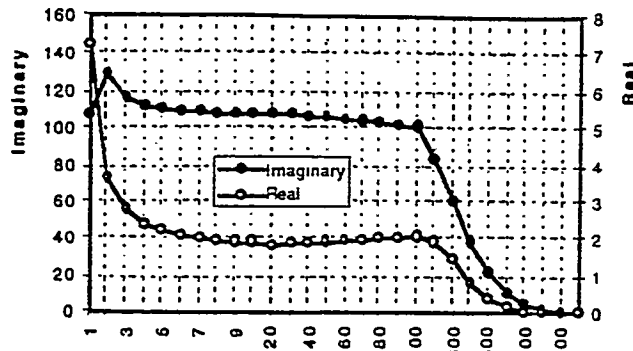


Figure 1. Longitudinal Coupling Impedance Z/n in ohm, versus harmonic number n

3.2 Transverse Coupling Impedance

There are four major contributions to the transverse coupling impedance. Like in the longitudinal case, also here the space charge contribution dominates in a low-energy storage ring. We have also contribution from the resistivity of the wall. By virtue of the deflection theorem, the beam-wall coupling impedance estimate can also be translated into an equivalent transverse coupling impedance. Figure 2 gives the estimate of the transverse coupling impedance for the low-energy NSNS storage ring.

3 INDIVIDUAL BUNCH INSTABILITIES

It is customary to divide these in the longitudinal, transverse and head-tail effects. We shall examine each of them below for the example of the NSNS storage ring described above. We like to point out that our case corresponds again to a low-energy storage ring operating well below the transition energy. Therefore results that are typical to high energy storage rings do not necessarily apply here.

3.1 Longitudinal Instabilities

There is a single long bunch. Coasting beam theory [4,6] is first applied by estimating the complex factor

$$U' - iV' = -i 2 e I_p \beta^2 (Z/n) / \pi \ln |E (\Delta E/E)_{FWHM}|^2 \quad (3)$$

where I_p is the bunch peak current and $\eta = \gamma_T^{-2} - \gamma^2$

For our case, taking the space charge contribution and an inductive wall contribution of $-i 20$ ohm as well as a resistive contribution of 3 ohm gives $U' = 1.1$ and $V' = 0.02$ which corresponds to a full momentum spread $\Delta p/p = 1.7\%$. Figure 3 shows the stability diagram in the (U', V') space for a cos-distribution [6]. The working point is

marked with a large black circle. It corresponds to a total bunch area of 10 eV-s. With this value the motion is stable.

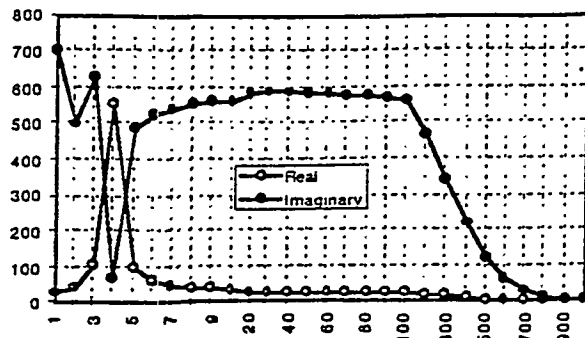


Figure 2. Transverse Coupling Impedance Z/n in kohm/m, versus harmonic number n

Even when the U' , V' parameters fall outside the coasting beam stability area, there are two other conditions that are to be satisfied in order for the motion to be unstable. One is the so-called Hereward condition [7], that is the ratio of the instability growth rate to the synchrotron frequency should be less than unit. In our case this is 0.084 which clearly shows very little consequences from the synchrotron motion, and thus the beam continues to be stable

The other condition deals with the fact that the coasting beam theory was developed assuming only one mode at the time, that is that neighboring coherent modes are completely decoupled from each other. This is satisfied only if the real frequency shift is sufficiently small compared to the revolution frequency. Unfortunately the real frequency shift is 3.5 times the revolution frequency so that several coherent modes are involved at the same time [8]. We do not have yet an understanding of this effect and whether there is a consequence to the beam stability.

3.2 Transverse Instability

Also in this case the method is the same. We first apply a coasting beam theory [9,10] stability condition given by

$$|Z_T| < E_0 \pi v \beta \gamma [|(n - v)\eta + \xi| (\Delta p/p) + \delta v] / e I_p R \quad (4)$$

$$= Z_{beam}$$

where E_0 is the proton rest energy, ξ the accelerator chromaticity, and δv the betatron tune spread from non linear elements like octupole magnets. We estimate also the growth rate of a potential instability in the limit of no Landau damping [5],

$$\tau^{-1} = I_p r_p \operatorname{Re}(Z_T) / e v \gamma Z_0 \quad (5)$$

For $n < 100$ the growth time is smaller than 0.2 ms which is considerably shorter than the synchrotron period of 1.2 ms, showing thus the possibility of fast coasting beam-like

instabilities. The stability condition (4) cannot be satisfied for $n < 100$ without an external tune spread. For the motion to be stable at all modes one requires $\delta v = 0.11$ which can be provided by octupole magnets. It is to be noted that the tune spread from the incoherent space-charge forces does not have a stabilizing effect on coherent oscillations.

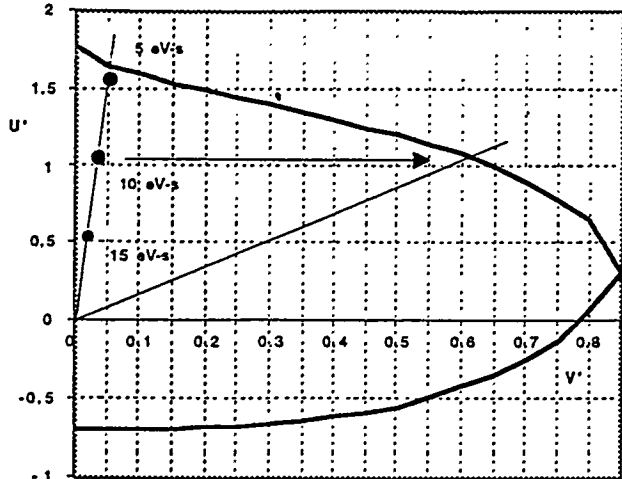


Figure 3. (U', V') stability diagram for cos-distribution

3.3 Head-Tail Effect

The only other concern left is the possibility of slow head-tail instabilities [11], for which the stability criterion (4) does not apply. This type of instability is caused by the transverse betatron motion coupled to the synchrotron motion. It may occur only when the growth rate is comparable or lower than the synchrotron frequency. The parameter of relevance is the accumulated betatron phase shift

$$\chi = 2\pi\zeta v f_0 \tau_L / \eta \quad (6)$$

where τ_L is the bunch length in time units, and f_0 is the revolution frequency. For the case of uncorrected chromaticity this quantity is positive and large (we are constantly below transition energy and $\zeta < 0$), ranging around 60. The head-tail mode numbers m which are stable, also in the absence of Landau damping, can be estimated from the condition $m < \chi / 2\pi$, which gives $m < 10$. Thus the head-tail instability is unlikely to appear in the accumulator ring.

4 INCOHERENT SPACE-CHARGE EFFECTS

The space charge effects are particularly important in NSNS, owing to the relatively low injection energy, and also the allowed low level of the beam loss. The maximum incoherent tune spread is estimated by,

$$\Delta v = N r_p / 2 B_f \beta^2 \gamma^3 \varepsilon \quad (7)$$

where N is the total number of particles, $r_p = 1.535 \times 10^{-18}$ m, and ε is the full unnormalized beam emittance which can be taken as 5 times the rms emittance. The bunching factor B_f is defined as the ratio of the average beam current over the peak current. To avoid arbitrary cuts and discontinuity of the distribution at the tail, we have adopted a square-cosine type of distribution with τ_L the total bunch length. The bunching factor for such a distribution can be easily estimated,

$$B_f = 0.5 \tau_L f_0 = 0.32 \quad (8)$$

We note that in the NSNS there is only one single bunch. The resulting tune spread for the NSNS is 0.2. In practice this value is expected to be lowered by the flattening effect of the longitudinal space charge forces. Moreover, a tune spread of about half the space-charge depression is needed to be created with octupoles to stabilize the beam against transverse coherent oscillations. The octupole polarity can be chosen in such a way the corresponding tune spread actually subtract from the space charge value yielding an overall spread of about 0.1.

Other two approaches can be considered to reduce further the tune spread. One is the use of a second harmonic RF system to flattened the distribution toward larger values of the bunching factor. The second method is to adopt the "painting" technique during injection to shape the beam toward a more rectangular transverse distribution. There are nevertheless concerns about the attainment of these flattened distributions since they can cause disruptive effects of coherent instability both in the longitudinal and transverse plane.

5 REFERENCES

- [1] J. Alonso, The NSNS Project, contribution to EPAC 96, Barcellona, Spain. June 1996.
- [2] A. Sessler and V.G. Vaccaro, Internal Yellow Report, CERN 67-2, Feb. 1967.
- [3] C.E. Nielsen et al., Proc. of Int. Conf. on High Energy Accel., 239, CERN 1959.
- [4] V.K. Neil and A.M. Sessler, Rev. Sci. Instr., 36, 429 (1965).
- [5] A.G. Ruggiero, W.T. Weng, S.Y. Zhang, AGS Internal Report, Brookhaven 1996. In preparation.
- [6] A.G. Ruggiero and V.G. Vaccaro, CERN - ISR - TH / 68-3, July 1968.
- [7] H.G. Hereward, Proc. of the 1975 ISABELLE Summer Study, vol. II, p. 555.
- [8] F. Sacherer, IEEE Trans. on Nucl. Sci., vol. NS-24, no. 3, 1393 (June 1977).
- [9] L.J. Laslett, V.K. Neil, A.M. Sessler, Rev. Sci. Instr., 36, 436, (1965).
- [10] K. Hubner, A.G. Ruggiero, V.G. Vaccaro, Proc. 7th Int. Conf. on High Energy Accel., Yerevan, p. 343 (1969).
- [11] C. Pellegrini, Nuovo Cimento, 64A, 477 (1969).



DISCLAIMER

This report was prepared as an account of work sponsored by an agency of the United States Government. Neither the United States Government nor any agency thereof, nor any of their employees, makes any warranty, express or implied, or assumes any legal liability or responsibility for the accuracy, completeness, or usefulness of any information, apparatus, product, or process disclosed, or represents that its use would not infringe privately owned rights. Reference herein to any specific commercial product, process, or service by trade name, trademark, manufacturer, or otherwise does not necessarily constitute or imply its endorsement, recommendation, or favoring by the United States Government or any agency thereof. The views and opinions of authors expressed herein do not necessarily state or reflect those of the United States Government or any agency thereof.